Predicting the impact of climate change on the area of wetlands using remote sensing

Nima Heidarzadeh
n.heidarzadeh@khu.ac.ir

Kharazmi University

Mahdiyeh Eghbal
Kharazmi University

Negar Esmaeili
Kharazmi University

Kaveh Panaghi
Head of Hydro-Meteorology Group at MG Consulting Engineering Company

---

Research Article

Keywords: Climate Change, scPDSI, SDSM, LARS-WG, Remote Sensing, MNDWI

Posted Date: July 24th, 2023

DOI: https://doi.org/10.21203/rs.3.rs-3178370/v1

Additional Declarations: No competing interests reported.

Version of Record: A version of this preprint was published at Theoretical and Applied Climatology on April 13th, 2024. See the published version at https://doi.org/10.1007/s00704-024-04969-9.

Predicting the impact of climate change on the area of wetlands using remote sensing

Nima Heidarzadeh, [a], Mahdiyeh Eghbal [b], Negar Esmaeili [c], Kaveh Panaghi [d]

a) Assistant Professor, Department of Civil Engineering, Engineering Faculty, Kharazmi University, Tehran, Iran.

b) M.Sc. in Environmental Engineering, Department of Civil Engineering, Engineering Faculty, Kharazmi University. Tehran, Iran.

c) M.Sc. in Environmental Engineering, Department of Civil Engineering, Engineering Faculty, Kharazmi University and PhD student of Environmental Engineering, Civil Engineering Department, Iran University of Science and Technology (IUST), Tehran, Iran.

d) Head of Hydro-Meteorology Group at MG Consulting Engineering Company, Tehran, Iran.

Address for Correspondence
*Nima Heidarzadeh,
Department of Civil Engineering, Engineering Faculty, Kharazmi University,
Tehran
Iran
Tel: +98-912-2279268
E-mail: n.heidarzadeh@khu.ac.ir

This research did not receive any specific grant from funding agencies in the public, commercial, or not-for-profit sectors.

Abstract

Climate change has been the main environmental challenge in recent years. In this research, the impact of climate change on the Arjan Wetland, Iran, has been investigated. The global climate models of canESM2 and hadGEM2 were used to predict the air temperature and precipitation for 2025-2066 in scenarios of RCP 2.6, 4.5, and 8.5. Temperature and precipitation data were downscaled using SDSM and LARS-WG software, respectively. Then, the wetland area was measured by processing the Landsat satellite images using the MNDWI algorithm. Forecast data were applied to estimate the wetland area for 2025-2066 and the scPDSI drought index. The results indicate that the estimated areas of the future period will slightly decrease; as a result, 90% of the areas in the years 2045-2066 are less than 800 hectares, and more than1100 hectares have not been dried in these years. The reduction of the area compared to the observation period is due to climate change and it shows the Arjan wetland is going towards drought. In 2039-2036, 2042, 2052, 2056-2058, and 2062, severe droughts will occur in wetlands under three scenarios with an area of less than 200 ha. Furthermore, the wetland will experience severe wet years in 2025, 2044, and 2045.

Keywords: Climate Change, scPDSI, SDSM, LARS-WG, Remote Sensing, MNDWI

1. Introduction

In recent years, industrialization and overuse of fossil fuels have raised global air temperature and changed the pattern of precipitation. Drought, one of the most important consequences of climate change, has long-term and undeniable environmental effects (Vrochidou et al. 2013). Wetlands are more sensitive to rainfall than other surface water sources due to their shallow depth. Analyzing the impact of climate change requires investigating the hydrological characteristics of wetlands. In this regard, the water volume change is inspected for at least three decades. Therefore, the water balance equation is usually used to calculate the difference in the volume of incoming and outgoing water (Sadeghi and Raisi Ardakani, 2018). Remote sensing (RS) is a low-cost tool that uses different algorithms to accurately classify wet and dry regions and calculate the wetland area. The general circulation model (GCM) and climate change scenarios, known as representative concentration pathways (RCPs), are standard tools for assessing future changes in rainfall regime, runoff, and temperature that dramatically affect wetland water budgets.

Previous studies indicate the increasing trends of precipitation and runoff in different regions such as Tonga Bhadra River, India (Meenu et al. 2013), Malaysia (Tan et al. 2017), and Lar Dam, Iran (Javaherian et al. 2021). Other researchers have also reported a reduction in runoff in several regions: British Columbia, Canada (Schnorbus and Cannon, 2014), Kermanshah, Iran (Rajabi et al. 2012; Salajegheh et al. 2016), and the Yarmouk River, Jordan, and Syria (Al-Shurafat and Abdullah, 2020). In contrast to these studies, Gebrechorkos et al. (2020) showed no significant precipitation trend in the Ethiopian Great River Basin.

One of the challenging concerns in climate change studies is how to convert large-scale climate data into local scale, known as downscaling. Researchers have applied several methods such as the statistical downscaling model (SDSM), long Ashton research station-weather generator (LARS-WG), and artificial neural network (ANN). These methods perform differently in estimating precipitation and temperature. Most researchers recommend the SDSM for temperature downscaling (Khan et al. 2006; Lopes, 2009; King et al. 2009; B.M. et al. 2012; Tukimat et al. 2019; Salajegheh et al. 2016). In addition, it has also been reported LARS-WG model is more efficient in precipitation downscaling (Lopes, 2009; King et al. 2009; Salajegheh et al. 2016; Shagega et al. 2019).

Identifying drought periods and runoff change regimes based on climatic variables/indices is also one of the critical issues in wetland climate change studies. The most important indices are the Palmer Drought Severity Index (PDSI), Standardized Precipitation Index (SPI), Standardized Runoff Index (SRI), Standardized Soil

Water Index (SSWI), Self-Calibrated PDSI (scPDSI), Original PDSI (orPDSI), Standardized Precipitation-Evapotranspiration Index (SPEI), and Standardized Precipitation Actual Evapotranspiration Index (SPAEI). Rezvanfar and Heidarzadeh (2017) used SPI, scPDSI, orPDSI, and SPEI drought indices to study the climate of the Arjan wetland in Iran. The results showed that the scPDSI had the best correlation with the reduction of wetland water volume. Ogunrinde et al. (2020) used the scPDSI to study the drought in the Niger River Basin from 1981 to 2015, with the maximum drought reported in 1998–2001. Based on their result scPDSI showed long-term hydrological drought of the Niger River with acceptable accuracy. Zhao et al. (2020) reviewed the North American watershed's climatic and hydrological drought periods. They used SPI to estimate meteorological drought and the Streamflow Drought Index (SDI) for hydrological drought. They anticipated that SPI would increase and decrease in the future, which is almost in line with the precipitation pattern. However, SDI indicated an extreme increase in drought in the coming years due to rising temperatures. Abbasiana et al. (2021) studied the drought in the Urmia Basin. They attributed the meteorological drought to the simultaneous occurrence of low precipitation and high temperatures. Accordingly, they recommendeda bivariate index called Precipitation-Temperature Deciles Index (PTDI). Rehana and Sireesha Naidu (2021) stated that univariate drought indices do not accurately reflect climate change drought. They used the SPAEI and three general circulation models to predict severe drought in the Krishna River Basin, India. In southern India, Satish Kumar et al. (2021) compared Drought Severity Index Gravity Recovery and Climate Experiment (GIACE-DSI), SPI, scPDSI, SPEI, Combined Climatological Deviation Index (CCDI), and GRACE Total Water Storage Anomalies (GRACE-TWSA) in all seasons during 2002–2016. The result shows a high correlation between GRACE-TWSA, GIACE-DSI, scPDSI, and CCDI. Lashkari et al. (2021) used the Power Dissipation Index (PDI) to estimate drought in arid and semi-arid regions of Iran to evaluate the impacts of precipitation changes. They found that PDI could demonstrably describe the annual drought in Iran.

Various innovative tools, such as RS and geographic information systems (GIS), have recently been widely applied to identify, monitor, and classify natural resources. Huang et al. (2011) used the Normalized Difference Vegetation Index (NDVI), the Normalized Difference Water Index (NDWI) algorithms, and the 5th band Landsat satellite band to simulate the water level of Cottonwood Lake Wetland in North Dakota from 1984 to 2009 (one image per year) and then to calculate the area of the wetland. Ghebrezgabher et al. (2016) used Landsat images and the Modified NDWI (MNDWI), NDVI, Voluntary Cooperation Program (VCP), and Soil-Adjusted Vegetation Index (SAVI) algorithms from 1970 to 2014 to increase the accuracy of Earth objects in Google Maps for the Eritrean region. They used MNDWI to determine the boundary between water and land. They reported 68 square kilometers of decrease in water level in the period. Sarp and Ozcelik (2017) also used Landsat images to analyze the Spatio-temporal changes of Boudoir Lake from 1987 to 2011. Support Vector Machine (SVM), MNDWI, NDWI, and Automated Water Extraction Index (AWEI) were applied in this study. The SVM with MNDWI was identified as the better method. The area of the lake reduced in 2000 to one-fifth of its area in 1987. Other studies also confirmed the better performance of MNDWI (Zhang et al. 2011; Gautam et al. 2015; Yang et al. 2011). Moreover, Li et al. (2021) used RS images from various methods, such as Comprehensive Drought and Waterlogging Index (CDWI), Shadow Difference Water Index (SDWI), MNDWI, Background Difference Water Index (BDWI), Total Column Water (TCW), Automated Water Extraction Index (AWEInsh, AWEIsh) and 2015 Water Index (2015WI) for Jiangsu Province, China. In these methods, BDWI with 97% correlation was the best, and MNDWI with 95% correlation was a reliable method. Furthermore, Wen et al. (2021) investigated different Thresholding Single Water Index image (TSWI) methods to detect surface water from land. The results showed that MNDWI was the best among NDWI, AWEI, and WI2015 methods. Cordeiro et al. (2021) also investigated the different methods such as MNDWI, NDWI, A robust Multi-Band Water Index (MBWI), Band 8, and Band 12 to identify pixels in inland waters based on multi-spectral satellite data; NDWI and MNDWI were the best methods, respectively.

This research investigates the effects of climate change on the Arjan wetland. It is conducted by forecasting the air temperature and precipitation data from 2025 to 2065 and calculating the drought index for the next period. Then, the wetland area in the future is calculated and compared with the observed area. After verifying the data, the temperature and precipitation were predicted using the two models of canESM2 and hadGEM2 and downscaled by SDSM and LARS-WG software in three RCP scenarios (2.6, 4.5, and 8.5). The drought was evaluated using the PDI, PNPI, and scPDSI from 1986 to 2018. The wetland area was estimated using the MNDWI algorithm on Landsat 5, 7, and 8 satellite images for 1986-2018. Finally, the relationship between wetland area and climatic parameters of the region was investigated to predict the wetland area for better management of water resources in the future.

2. Materials and methods

2.1. Study area

The Arjan Wetland is located in Fars province, Iran (Figure 1). The Arjan plain has an average temperature of 13.9 °C with an average annual precipitation of 671.4 mm. The maximum watershed area of the wetland has been 1663 hectares, with water depth reaching 1 meter in some areas. Its maximum volume was 43 million cubic meters in 2011 (Sadeghi and Raisi Ardakani, 2018). With an approximate area of 90 square kilometers and a height of 1990 meters, it is part of the Arjan-Parishan biosphere reserve. Due to the importance of tourism, the environment, and the creation of job opportunities for its inhabitants, reducing the water level in summer has been a paramount concern. Rain and snow in its enclosed basin are the only inflow water sources for the Arjan wetland (National Commission for UNESCO-Iran, 2017).

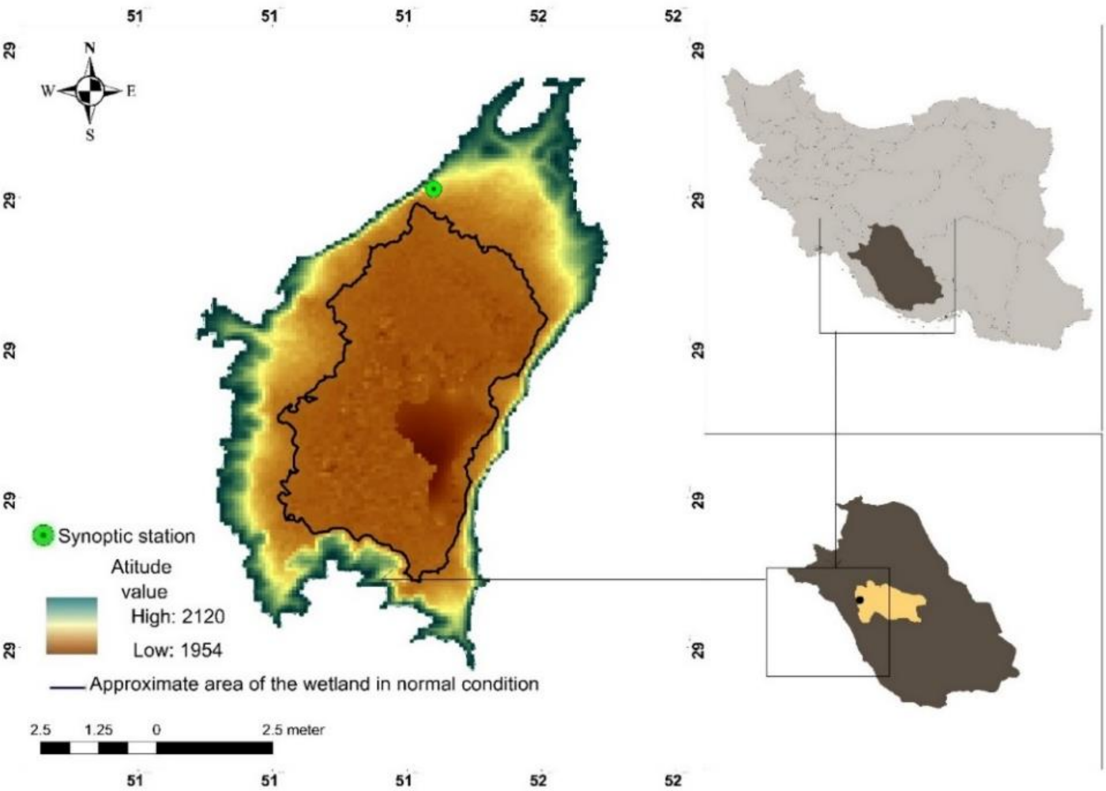

Fig.1 The geographical location of the Arjan wetland in Iran

2.2. Data

Minimum and maximum temperature and daily precipitation data were collected from the Arjan wetland evaporation station provided by the Fars Regional Water Department of Iran. Monthly temperature and precipitation data for the historical and next period in three scenarios of RCP 2.6, 4.5, and 8.5, was received from the Earth System Grid Federation (ESGF) website. Moreover, National Centers for Environmental Prediction (NCEP), historical, and RCP daily data of the canESM2 model were obtained from the model support website (climate-scenarios.canada.ca). In addition, Landsat satellite images were downloaded from the U.S. Geological Survey website from 1986 to 2018.

2.3. Methods

As the location of the wetland is located in a semi-arid region, the canESM2 model was used based on the previous researchers' suggestion (Javaherian et al. 2021; Al-Shurafat and Abdullah, 2020; Chim et al. 2021; Zhao et al. 2020, Tukimat et al. 2019). The Hadley Center Global Environment Model version 2 (hadGEM2) was also used to improve the results (Morid et al. 2020; Almagroa et al. 2020; Khazaei et al. 2019). The selected scenarios are RCP 2.6, 4.5, and 8.5, which are optimistic, moderate, and pessimistic, respectively. The large-scaled daily temperature and precipitation data of the CanESM2 model in RCP scenarios 2.6, 4.5, and 8.5 were respectively downscaled by SDSM and LARS-WG for 2025–2065. Because many researchers reported that the SDSM and LARS-WG models are more suitable for downscaling daily temperature and precipitation, respectively (Salajegheh et al. 2016; Sobhani et al. 2014; Dehghan et al. 2014; and King et al. 2009).

2.3.1. Validation

The root-mean-square error (RMSE) and relative error of observational data (E) were used to compare downscaled predicted data with the observations in the same period.

$$RMSE = \sqrt{\frac{\sum_{i=1}^{n}(X_i - Y_i)^2}{n}} \qquad (1)$$

$$E = \frac{2}{n}\sum_{i=1}^{n}\frac{|X_i - Y_i|}{X_i + Y} \qquad (2)$$

where xi is the average monthly temperature or precipitation, yi is the average monthly predicted temperature or precipitation, and n is the number of months (n=12).

2.3.2. Drought intensity

To evaluate the drought intensity, three drought indices of PNPI (Mir Yaghoubzadeh and Khosravi, 2018; Mohamadian et al. 2010; Mahmoudi et al. 2019; and Karimi et al. 2010), PDI (Lashkari et al. 2021; Mir Yaghoub Zadeh and Khosravi, 2018; Mohammadian et al. 2010; and Karimi et al. 2010), and scPDSI (Almagroa et al. 2020; Satish Kumar et al. 2021; Mir Yaghoubzadeh and Khosravi, 2018; Rezvanfar and

Heidarzadeh, 2017; and Huang et al. 2011) were applied from 1984 to 2018. The DIP software was used to calculate the PNPI and PDI (Morid et al. 2007). This software receives precipitation monthly data and provides an output on a monthly, seasonal, and annual basis. R programming software version 4.0.2 was also used to estimate the scPDSI (Wells et al. 2004).

2.3.3. Calculation of the wetland area

As the MNDWI is the best algorithm proposed by previous studies for classifying wet and terrestrial areas, it was implemented on the Landsat 5, 7, and 8 satellite images to calculate the wetland area for each year. Each satellite image represents one year and corresponds to the summer months of July, August, and September (Sarp and Ozcelik, 2017; Ghebrezgabher et al. 2016; Yang et al. 2011; Zhang et al. 2011; Cordeiro et al. 2021; Li et al. 2021; Wen et al. 2021).

2.4. Modeling changes in wetland area by drought indices

The area of the wetland has been calculated using ArcGIS 10 software. After computing the drought indices for the corresponding years for available satellite images, linear and non-linear regression have been used to find the highest correlation between drought indices and wetland areas as described below.

2.4.1. Simple linear regression

To evaluate the individual effect of climate change without direct human influence, the outlier data between 2013 and 2018 were not considered. During this period, a part of the wetland water has been used for agriculture and then causes disturbances in the natural wetland area. Moreover, two different annual periods were assessed to find the best one for evaluating the simple linear model efficiency. The first period is the common Julian year (JY) and the second is the suggested AD year as described below. The model individually uses the drought indices and precipitation calculated for both mentioned periods. Then, the wetland area for the current year was linearly modeled resulting in the drought indices and precipitation. AD year starts from August of the previous year to July of the current year.

2.4.2. Non-Linear regression

In the study of Mohseni et al. (1998), a four-parameter non-linear function was used to estimate the river flow temperature by utilizing air temperature. Since wetland water evaporation depends on the water temperature, a modified relationship was proposed to calculate the wetland area as shown in Eq. (3).

$$A_S = A_{\min} + \frac{A_{\max} - A_{\min}}{1 + e^{\gamma(\beta - scPDSI)}} \qquad (3)$$

where AS is the wetland area, scPDSI is the self-calibrated Palmer Drought Severity Index, Amin and Amax are the minimum and maximum wetland areas in the observational data, respectively, γ is a slope at the turning point, and β is the wetland area at the turning point. There are 30 corresponding data for AS and scPDSI in this study. To obtain γ and β values, the known parameters were replaced in the equation and were solved to minimize the RMSE and the Nash-Sutcliffe model Efficiency (NSE) by a trial-error procedure. Equations 4 and 5 were used to acquire the percentage of reliability of this correlation method.

$$NSE = 1 - \frac{\sum_{i=1}^{n}(A_{si} - A_{obsi})^2}{\sum_{i=1}^{n}(\overline{A}_{obs} - A_{obsi})^2} \qquad (4)$$

$$RMSE = \sqrt{\frac{\sum_{i=1}^{n}(A_{si} - A_{obsi})^2}{n}} \qquad (5)$$

where A_S is the wetland area (via Eq.3), and Aobs is the wetland area calculated by the ArcGIS software as explained before.

2.4.3. Linear regression with modified WWAI

The Wetland Water Area Index (WWAI) using PDSI was developed by Huang et al. (2011) in the study of Cottonwood Lake in North Dakota. A modified version of WWAI was used to predict the area of the Arjan wetland in the present study by replacing the scPDSI with the PDSI. Since the wetland's area does not completely depend on precipitation and temperature in the current year and precipitation in the previous year has accumulated, the cumulative scPDSI (scPDSICUM) was calculated which can show a better correlation than scPDSI. Nevertheless, since small changes are not expressed well, a weighting factor (Wi) should be defined with a range of 0 –1.

$$W_i = \frac{scPDSICUM_i - scPDSICUM_{\min}}{scPDSICUM_{\max} - scPDSICUM_{\min}} \qquad (6)$$

where scPDSICUMi is the cumulative scPDSI, and scPDSICUMmin and scPDSICUMmax are the minimum and maximum cumulative scPDSI, respectively.

When scPDSICUM is close to the minimum, W is nearly zero, indicating that the previous conditions were arid. When scPDSICUM is close to maximum, W is approximately equal to one, indicating that previous conditions were very wet. W values were calculated to obtain the area of the Arjan wetland after computing the cumulative drought index. Moreover, the scPDSICUM was divided into three classifications: scPDSICUMi <-10, -10 < scPDSICUMi <-5, and scPDSICUMi >-5. As Huang's study (Huang et al. 2011), this method requires five parameters (a, b, c, d, e) obtained by trial and error and needs calibration to predict the wetland area. Therefore, it is necessary to proceed according to the flowchart in Figure 2.

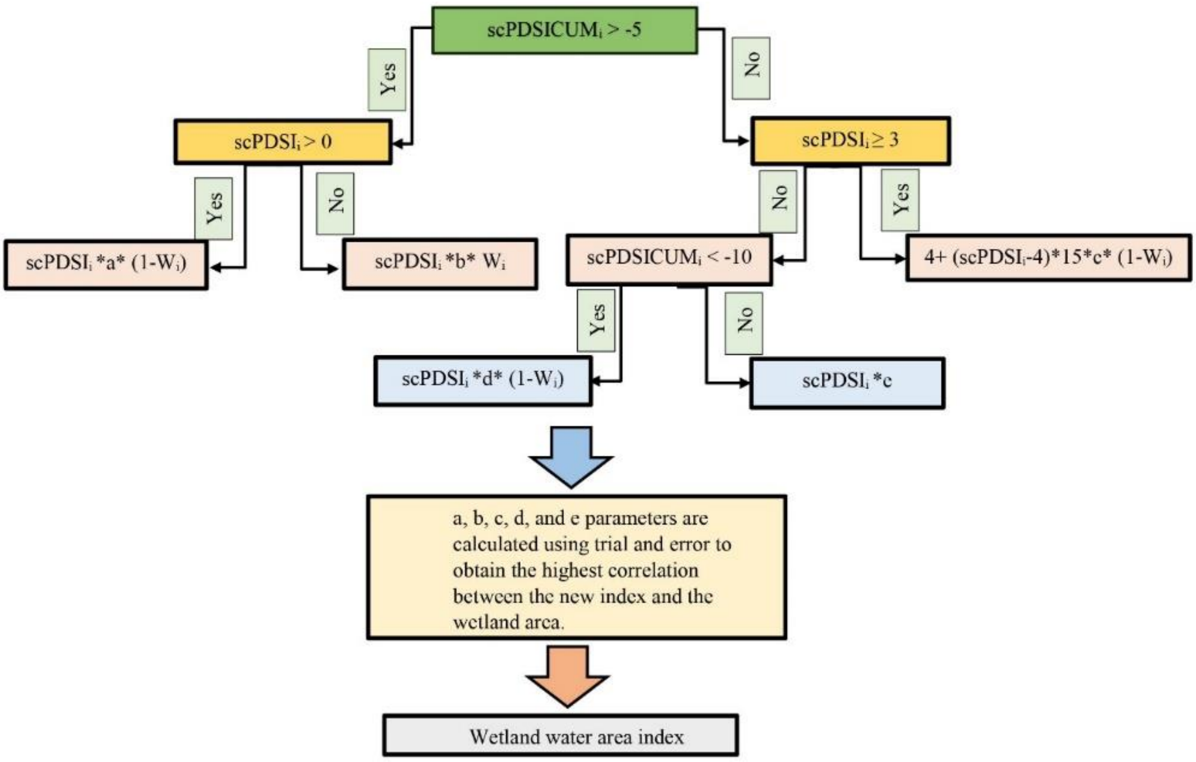

Fig.2 The steps of forming the wetland water level index

3. Results

3.1. Predicting air temperature

Figure 3(a) shows the annual maximum, minimum, and average temperature in the RCP 2.6, 4.5, and 8.5 for the historical and future periods. As indicated in Figure 3(a), the maximum temperature under RCP2.6 has reached 23.3˚C from 22.4 ˚C with an average slope of 1.5%. It means that the temperature has increased by 1.1 ˚C on average. In addition, according to RCP4.5 and 8.5, the maximum temperature increased with an average slope of 4.2% and 6.4%, and the temperature increased by 2.1 ˚C and 3.3˚C on average, respectively. Based on RCP 2.6, the annual minimum temperature has increased from 9.9 with an average slope of 1.6% and is expected to reach 10.9 in 2065. The minimum temperature has also increased by 1.7 ˚C under the RCP 4.5 and 3.1 ˚C under the RCP 8.5 scenarios. Figure 3(a) also indicates the amount of average annual temperature increase, which is acquired from the average maximum and minimum temperatures.

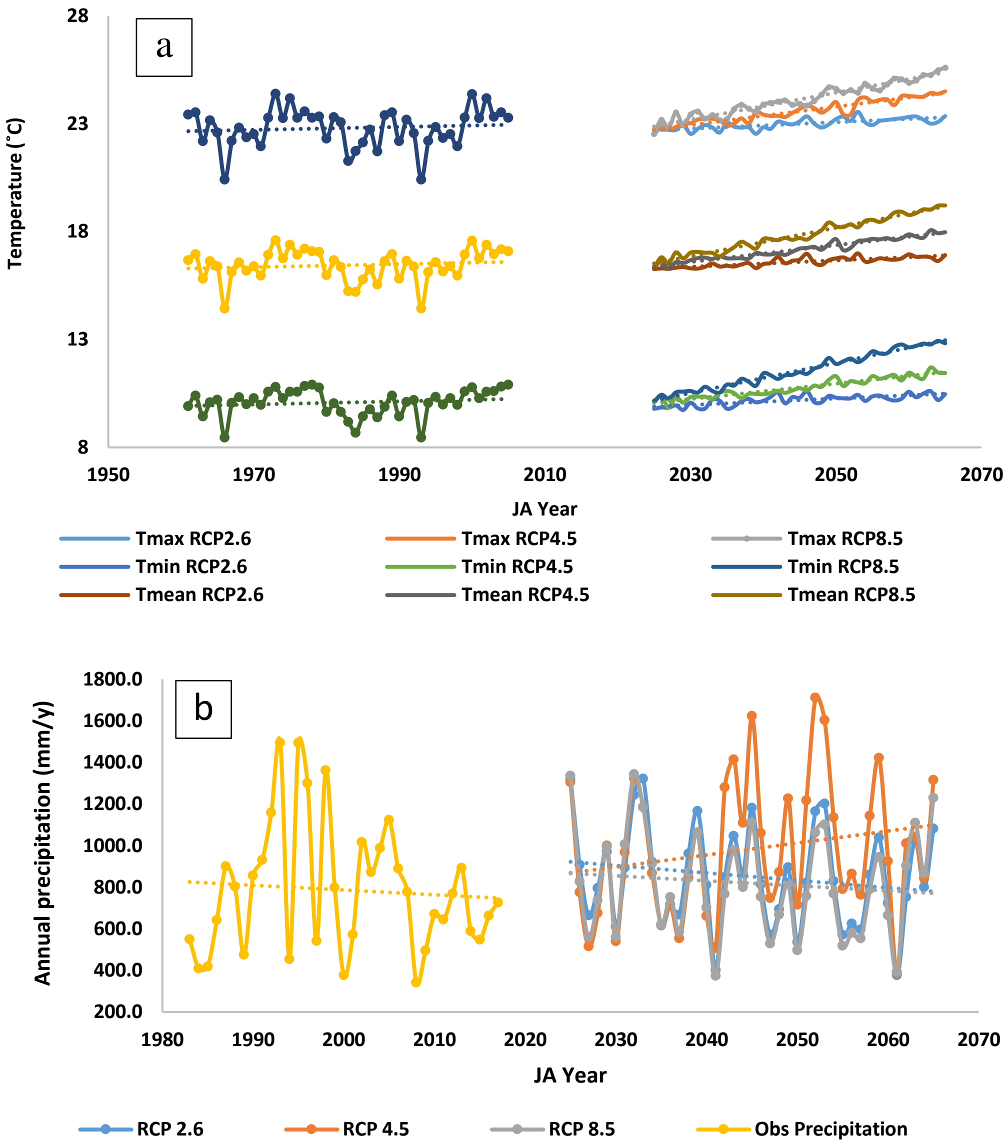

Fig.3 Air temperature (a) and annual precipitation (b) changes of the Arjan wetland in the observation and future periods, the minimum, maximum, and average annual

3.2. Predicting precipitation

Figure 3(b) demonstrates the results of precipitation predictions in the past and future. Table 1 also presents the statistical analysis of the predicted precipitation data for the future in different scenarios compared to the observed data using the t-test results. The average future precipitation in the three scenarios is higher than the average of the observed values.

According to Table 1, as the p-value for RCP2.6 and RCP8.5 were greater than 0.05, no significant correlation between precipitation data and observed precipitation was found, and only in RCP 4.5, the p-value was 0.029, which showed a meaningful correlation. The down-scaled precipitation in the future does not show a considerable increasing or decreasing trend compared to the observation period. However, the predicted precipitation under the three scenarios does not have the same trend. Similar results were presented in the research of Zhao et al. (2020), and Rezvanfar and Heidarzadeh, (2017). In Figure 3(b), the slope of precipitation changes under RCP 4.5 in the years 2025 to 2065 is positive (+0.09). While the predicted precipitation slope under RCP 2.6 and RCP 8.5 scenarios during 2025-2065 are -3.3 and -1.9, respectively. Since precipitation extremes are critical in water resources management, it is essential to specify them. Very low precipitation will occur in 2041 and 2060 under all three scenarios, and very high precipitation will happen in 2043, 2045, 2052, 2053, and 2059 under RCP 4.5. Based on the results of three future scenarios, the lowest precipitation will occur in 2041 and 2061 at about 380 mm per year compared to 340 mm in the observation period.

Table 1. The t-test results for comparing predicted precipitation under RCP scenarios with observational data (mean 786 and standard deviation 311 mm per year)

Scenarios	Mean	Standard deviation	P-value	T-value
RCP2.6	824	233	0.532	-0.63
RCP4.5	933	310	0.029	-2.23
RCP8.5	821	241	0.571	-0.57

3.3. Prediction of dry and wet years using drought indices

The drought was analyzed by calculating three indices of PNPI, PDI, and scPDSI. Figure 4 shows that the intensity of drought is not the same for these indices in each year; this could be due to the difference in the analysis of climatic parameters in each index. However, similar drought periods can be seen in all three indices including 1991 to 1997, 1983 to 1985, and 2008 to 2010. The results of PNPI and scPDSI seem better while the scPDSI usually indicates the drought period with a one-year delay. It is probably because of the different definitions of the indices since the PNPI is based on meteorological drought, while the scPDSI is applicable for hydrological drought estimation and is measured based on soil moisture. Hydrological drought may occur after meteorological drought. In the last ten years, scPDSI has estimated drier years than PNPI and

PDI; this could be due to the use of the temperature in this index which is an increase in the average annual temperature compared to the previous year(s) showing more drought, despite the almost acceptable precipitation. For example, the PNPI shows severe draught in 2004 while this year is considered a normal year based on the scPDSI. In addition, the year 2001 is a normal year based on both the PNPI and PDI indices, unlike the severe drought calculated by the scPDSI. Like our results, Zhao et al. (2020) also reported more intense drought due to increasing temperature.

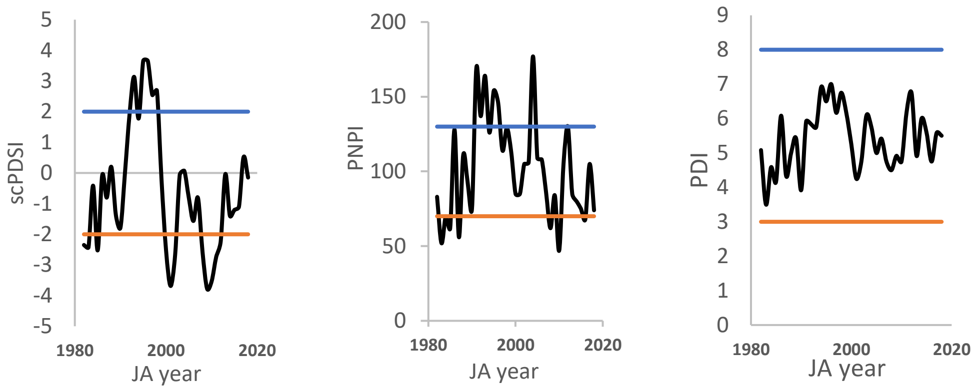

Fig.4 Changes in the drought indices of Arjan wetland during the years 1982-2018 (In all figures, the orange lines show moderate drought, and the blue lines show moderate wet)

3.4. Changes in the area of the Arjan wetland

Figure 5 shows the selected satellite images in summer between 1986 and 2018. The wetland area in summer is also shown in Figure 5 using the MNDWI algorithm on Landsat satellite images. In recent years, the wetland area has significantly decreased and it was almost dried in 2018. The results showed the scPDSI is more accurate than the PNPI and PDI drought indices to estimate the Arjan wetland area. As seen in Figure 4 the scPDSI shows more drought than other indices in recent years so it can be more reliable. The first reason is the use of both temperature and precipitation, and the second is the use of the climate data of the previous year in calculating this drought index. These results confirm that the wetland area for each year is also affected by both precipitation and the area in the previous year. Similar findings were reported by Rehana and Sireesha Naidu (2021), Abbasiana et al. (2021), and Zhao et al. (2020).

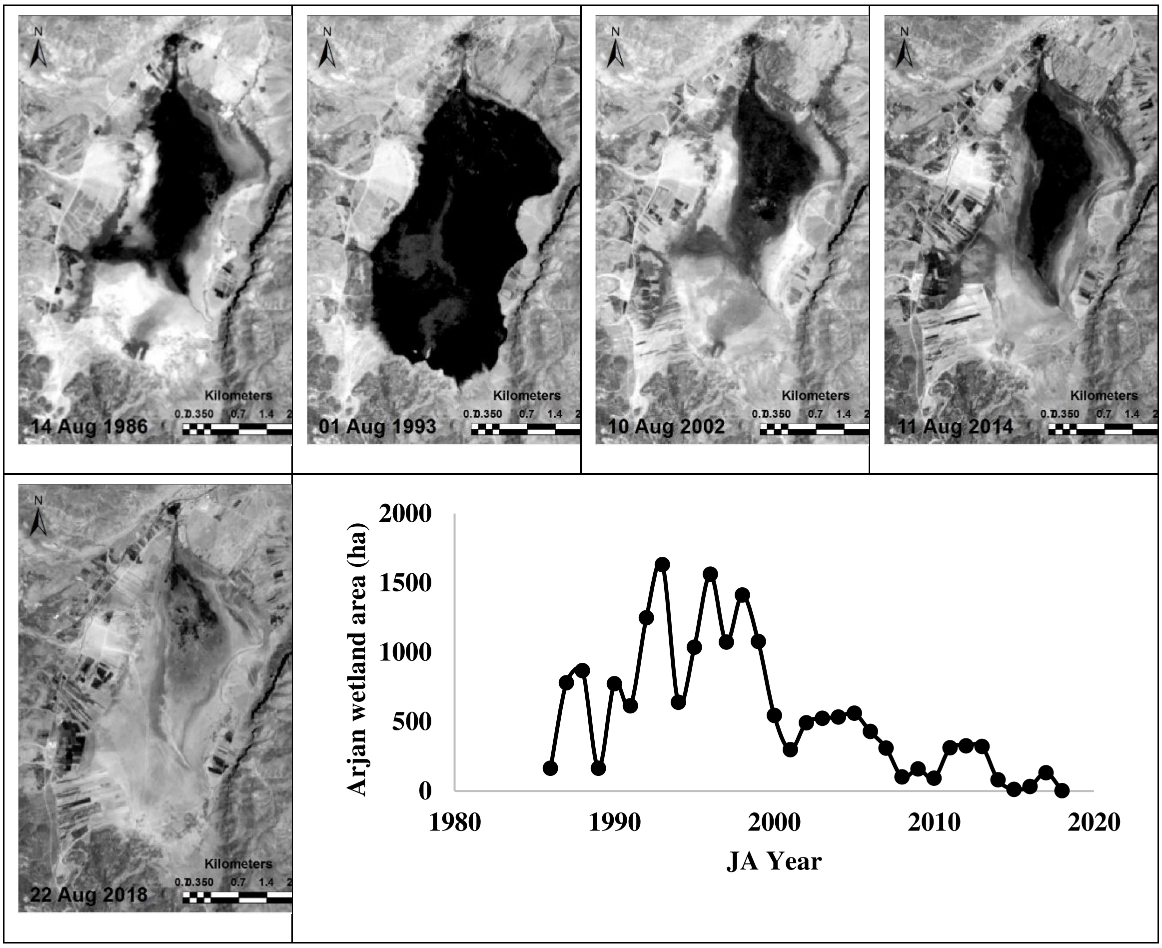

Fig.5 Selected satellite images and the area changes of the Arjan wetland

3.5. Modeling level changes

3.5.1. Simple linear regression

Table 2 shows the result of the simple linear regression between different climatic parameters and the Arjan wetland area. As indicated in Table 2, the PDI has no significant correlation with the Arjan wetland area. Although this index was used and confirmed by Lashkari et al. (2021), it was not suitable for this research. Based on the study of Mahmoudi et al. (2019) for the PDI, if the duration of the statistical period is short, this index will not describe drought conditions well. Despite the approval of many studies, such as Mahmoudi et al. (2019), Miryaghoubzadeh et al. (2019), and Karimi et al. (2010), the PDI was not compatible with modeling the area of the Arjan wetland, whereas scPDSI correlates well. Because the PNPI and PDI are univariate indices rather than the scPDSI. Single-variable drought indices seem not suitable for describing drought under climate change (Rehana and Sireesha Naidu, 2021; Abbasian et al. 2021; Zhao et al. 2020). However, all drought indices as well as precipitation demonstrate a better correlation with AD year than JA year. It is suggested that assuming AD year can be a suitable choice for such modeling. Table 2 also indicates the correlation coefficient of scPDSI of AD year and scPDSI of JY year are higher than in the rest of the parameters. Since the scPDSI of the AD year is higher than the scPDSI of the JY, the scPDSI of the AD year is selected for the non-linear regression in the next step.

Table 2. Coefficient of determination (R^2) of the linear regression between different climatic parameters and the Arjan wetland area in the past period

Climatic parameter		Period in concern	R^2
Precipitation		JY	0.29
		AD	0.51
Drought index	PDI	JY	0.2
		AD	0.32
	PNPI	JY	0.28
		AD	0.46
	scPDSI	JY	0.67
		AD	0.76
		Summer average	0.57

The final equation of linear regression scPDSI of the AD year for Arjan wetland shows in Equation 7.

$$A_i = 175.85(scPDSI_i) + 725.7 \qquad (7)$$

3.5.2. Non-linear regression

After using observational data, γ, β, NSE, and RMSE were obtained through a trial-and-error procedure using Eq. (3) and the scPDSI as the independent variable, which were 0.59, 0.79, 206.91, and 0.78, respectively, yielding Eq. (8). The NSE value shows a proper efficiency of this method but it did not significantly increase compared to linear regression. Figure 6(a) also shows the areas calculated by Eq. (8).

$$A_s = 92 + \frac{1541}{1+e^{0.59(0.79-scPDSI)}} \qquad (8)$$

Figure 6(a) illustrates that the scPDSI is a reliable model to estimate the wetland area, especially in the years with low precipitation.

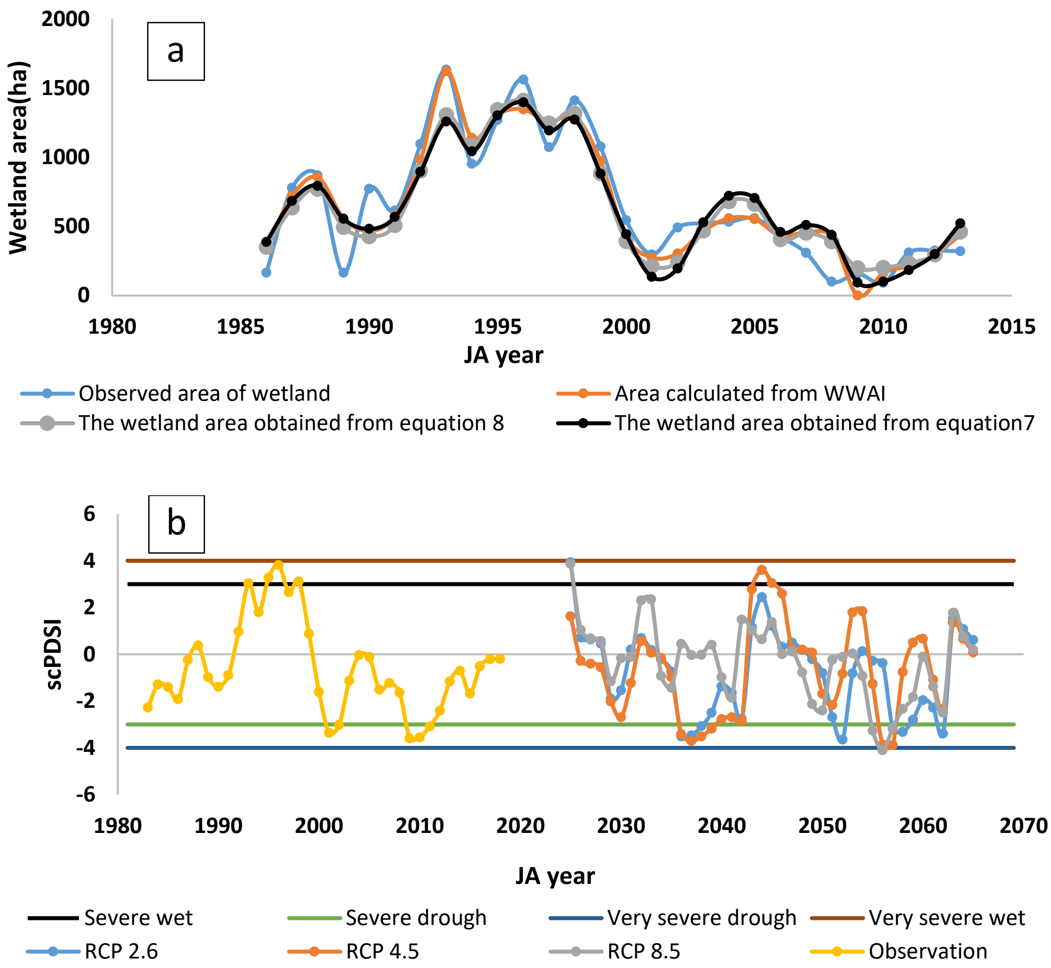

Fig.6 Comparison of the observed wetland area with the area obtained from equation 7, 8, and the area modeled by the WWAI (a) and scPDSI changes of Arjan wetland during the years 1983-2065 (b)

3.5.3. Linear regression with the modified WWAI

The values obtained for the unknown coefficients (a, b, c, d, e) obtained by trial and error equal 8.5, 3.2, -1.6, 6.7, and 2.3, respectively. The linear regression of the wetland water area index using the computed coefficients compared to the observed area showed that the R2 is equal to 0.88, which indicates a significant correlation. Figure 6(a) compares the area modeled by the modified WWAI with the observed area.

3.6.1. Calculation of scPDSI

Before estimating the wetland area, it is necessary to calculate the scPDSI for RCPs 2.6, 4.5, and 8.5. As seen in Figure 6(b), in 2025 and the years 2044-2045 will experience severe wet under three scenarios. Whereas there are three periods of severe drought including 2036-2039 2052, 2055-2058, and 2062. However, the drought in 2056 will be very severe under RCP 8.5. As seen in Figure 6(b), the number of extremely wet years in the observation period is 14%, whereas it will be 6% in the future. However, our estimations indicate that the number of severe drought years will not significantly change compared to the observation period, showing the decreased domain of changes compared to the past due to the longer period. Moreover, the trend of the scPDSI in scenarios RCP 2.6 and 8.5 is decreasing similar to the past period whereas RCP 4.5 slightly experiences an increasing pattern. A similar pattern can be observed for precipitation shown in Figure 3(b). Scenarios RCP 2.6 and 8.5, and the past period have a slightly decreasing trend in contrast with RCP 4.5 with a drastically increasing trend. Hence, it can guide us that precipitation has a lower effect on the scPDSI than temperature.

3.6.2. Estimation of wetland area in the future period using linear regression

As predicted by the simple linear regression method (Figure 7(a)), the wetland area will be under 200 ha and near zero for many years. In this method, the minimum and maximum area of the wetland were respectively predicted in 2062 (5 ha) and 2025, and 2044 (1400 ha).

3.6.3. Estimating the area of wetland in the future period using non-linear regression

Figure 7(b) shows that the non-linear regression for four years (2037, 2052, 2056, and 2057) has estimated an area below 200 ha, the lowest for 2056 with 173 ha. Comparing the observed area with this model (Figure 6(b)), the modeled area is over-estimated than the observed area in severe drought years such as 2008-2010. Therefore, it is likely that the areas that will report in the future in these years will be less than predicted in this method. The maximum area predicted according to this method will be roughly 1400 ha and it will happen in 2025 and 2044. Except for the minimum wetland areas mentioned above, the whole pattern of this method is similar to the linear model.

3.6.4. Estimating the wetland area in the future period using linear regression with the modified WWAI

The results of estimating the wetland area in the future period using the linear regression with the modified WWAI are shown in Figure 7(c). The minimum area of Arjan wetland in 2036 is estimated to be 22 ha. In addition, the maximum area in 2045 is 1610 ha, then in 2044 and 2025 with 1400 ha. The mentioned modeling of the wetland area are valid for the conditions without the other anthropogenic effects. As mentioned before, during 2014–2018, the wetland area decreased to less than 200 ha, which could be due to water abstraction for agriculture or other anthropogenic factors.

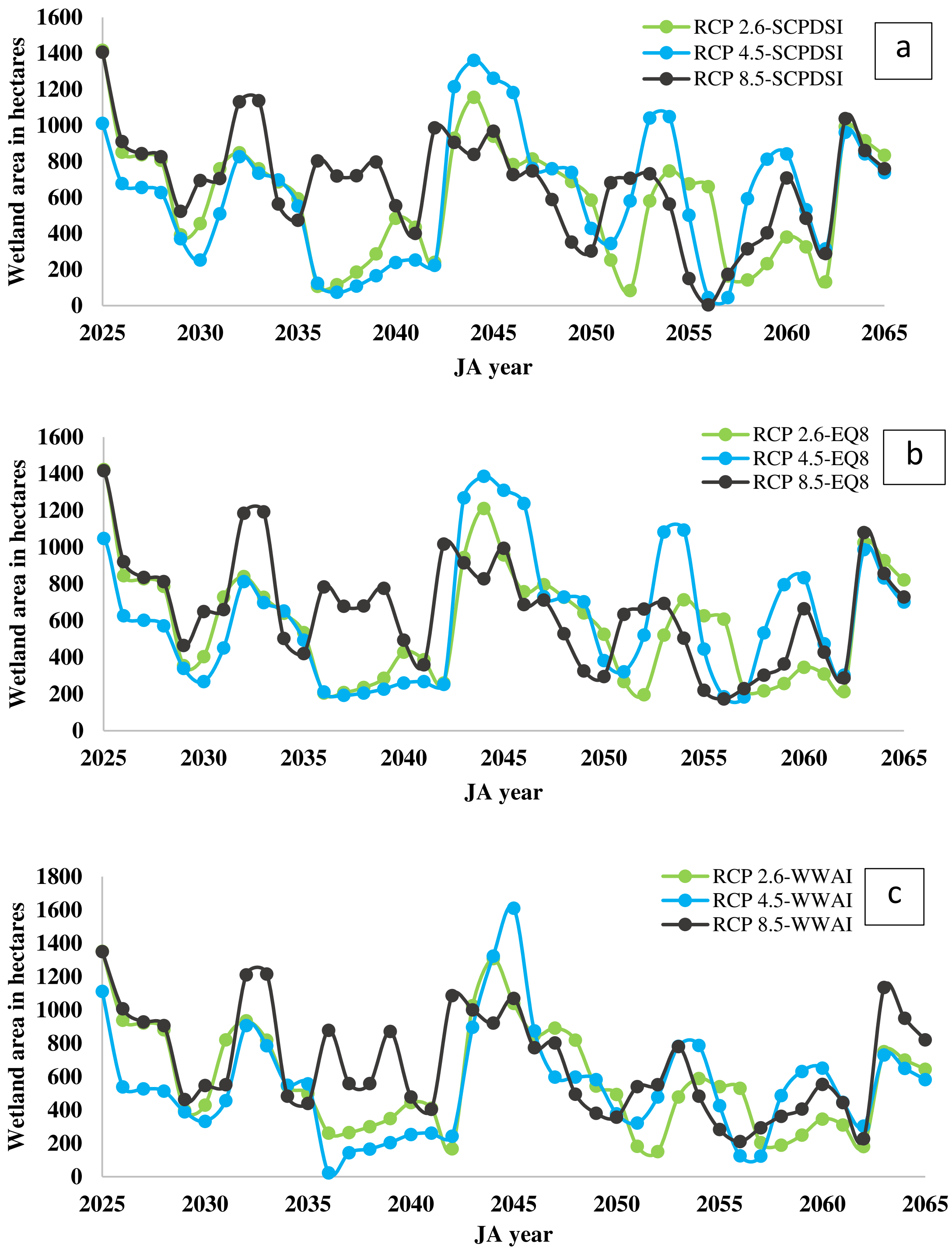

Fig. 7 Changes in the area of Arjan wetland during the years 2025-2065 according to a) the linear regression, b) the non-linear regression, and c) the modified WWAI model

4. Conclusions

This study tried to assess the climate change effect on the water budget in a natural wetland, especially in terms of wetland area.

Temperature evaluation from 2025 to 2065 under RCP 2.6, 4.5, and 8.5 scenarios revealed that the temperature increased by 1˚C, 1.7 ˚C, and 3.1 ˚C compared to the average historical value, respectively. Moreover, the precipitation for the mentioned period shows a small increasing or decreasing trend compared to the observation period.

Comparing drought indices of the PNPI and scPDSI showed that since 2000, the PNPI had estimated normal or wet years, while the scPDSI had estimated drought or normal years. As this index uses both temperature and precipitation to estimate drought conditions, it seems more reliable for modeling the wetland area. This fact was proved by comparing all three drought indices during the simple linear modeling of the wetland area.

The modeling of the Arjan wetland area in the future period was conducted by the scPDSI using three methods of simple linear, non-linear, and modified WWAI. Results showed that if the future period is divided into two parts, including 2025-2045 and 2045–2065, 90% density of modeled areas in the second period has less than 800 ha. Moreover, no areas are larger than 1100 during this period. It indicates that the major effect of climate change is significantly increased temperature for the mentioned period. The modeling also reveals that the Arjan wetland experiences severe droughts, an area below 200 ha, in years from 2036 to 2039 and 2042, 2052, 2058-2056, and 2062. Furthermore, the wetland will severe wet years 2025, 2044, and 2045.

However, this result holds if the Arjan wetland is affected only by climate change. These results are not valid when anthropogenic factors are also involved in this basin. If water is used for agriculture, the Arjan wetland may be entirely dried, much earlier than 2065, making its restoration so costly.

5. References

Abbasian, M.S., Najafi, M.R., Abrishamchi, A., 2021. Increasing risk of meteorological drought in the Lake Urmia basin under climate change: Introducing the precipitation–temperature deciles index. J. Hydrol. 592. https://doi.org/10.1016/j.jhydrol.2020.125586

Abdulla, F., Al-Shurafat, A.W., 2020. Assessment of the Impact of Potential Climate Change on the Surface Water of a Trans-boundary Basin: Case Study Yarmouk River, in: Procedia Manufacturing. https://doi.org/10.1016/j.promfg.2020.02.219

Almagro, A., Oliveira, P.T.S., Rosolem, R., Hagemann, S., Nobre, C.A., 2020. Performance evaluation of Eta/HadGEM2-ES and Eta/MIROC5 precipitation simulations over Brazil. Atmos. Res. 244. https://doi.org/10.1016/j.atmosres.2020.105053

Al-Shurafat, A.W.S., Abdullah, A.F., 2016. The spatial and temporal simulation of the hydrological water budget for Yarmouk river basin under current and projected future climate. Master thesis, Jordan University of Science and Technology, Jordan.

Muleneh, F., Melesse, A.M, Romano, E., Volpi, E. and Fiori, A., 2012. Statistical Downscaling of Precipitation and Temperature for the Upper Tiber Basin in Central Italy. International journal of water sciences. https://doi.org/10.5772/52890

Chim, K., Tunnicliffe, J., Shamseldin, A., Chan, K., 2021. Identifying future climate change and drought detection using CanESM2 in the upper Siem Reap River, Cambodia. Dyn. Atmos. Ocean. https://doi.org/10.1016/j.dynatmoce.2020.101182

Cordeiro, M.C.R., Martinez, J.M., Peña-Luque, S., 2021. Automatic water detection from multidimensional hierarchical clustering for Sentinel-2 images and a comparison with Level 2A processors. Remote Sens. Environ. 253. https://doi.org/10.1016/j.rse.2020.112209

Dehghan, Z., Fathian, F., Eslamian, S., 2014. Comparative Assessment of SDSM, IDW and LARS-WG Models for Simulation and Downscaling of Temperature and Precipitation. J. of Water and Soil. Vol. 29, No. 5, Nov.-Dec. 2015, p. 1376-1390. (In Persian)

Gautam, V.K., Gaurav, P.K., Murugan, P., Annadurai, M., 2015. Assessment of Surface Water Dynamicsin Bangalore Using WRI, NDWI, MNDWI, Supervised Classification and K-T Transformation. Aquat. Procedia 4. https://doi.org/10.1016/j.aqpro.2015.02.095

Gebrechorkos, S.H., Bernhofer, C., Hülsmann, S., 2020. Climate change impact assessment on the hydrology of a large river basin in Ethiopia using a local-scale climate modelling approach. Sci. Total Environ. 742. https://doi.org/10.1016/j.scitotenv.2020.140504

Ghebrezgabher, M.G., Yang, T., Yang, X., Wang, X., Khan, M., 2016. Extracting and analyzing forest and woodland cover change in Eritrea based on landsat data using supervised classification. Egypt. J. Remote Sens. Sp. Sci. 19. https://doi.org/10.1016/j.ejrs.2015.09.002

Huang, S., Dahal, D., Young, C., Chander, G., Liu, S., 2011. Integration of Palmer Drought Severity Index and remote sensing data to simulate wetland water surface from 1910 to 2009 in Cottonwood Lake area, North Dakota. Remote Sens. Environ. 115. https://doi.org/10.1016/j.rse.2011.08.002

Javaherian, M., Ebrahimi, H., Aminnejad, B., 2021. Prediction of changes in climatic parameters using CanESM2 model based on Rcp scenarios (case study): Lar dam basin. Ain Shams Eng. J. 12. https://doi.org/10.1016/j.asej.2020.04.012

Karimi, V.A., Habibnejhad Roshan, M., Abkar, A.J., 2010. Investigation of meteorological drought Indixes in Mazandaran synoptic Stations. Irrigation and water engineering scientific research quarterly. Number 2, fall 2010, 15-25 pp. (In Persian)

Khan, M.S., Coulibaly, P., Dibike, Y., 2006. Uncertainty analysis of statistical downscaling methods. J. Hydrol. 319. https://doi.org/10.1016/j.jhydrol.2005.06.035

Khazaei, M.R., Tahsinzadeh, N., Sharafati, A., 2019. Uncertainty Investigation of Precipitation and Temperature Scenarios for the Sira Basin under Climate Change Impact. Iran-Watershed Management Sci & Eng. Vol. 13, No. 46, Fall 2019. (In Persian)

King, L., Solaiman, T., Simonovic, S.P., 2009. Assessment of climatic vulnerability in the Upper Thames River Basin. Department of Civil and Environmental Engineering, The University of Western Ontario.

Lashkari, A., Irannezhad, M., Zare, H., Labzovskii, L., 2021. Assessing long-term spatio-temporal variability in humidity and drought in Iran using Pedj Drought Index (PDI). J. Arid Environ. 185. https://doi.org/10.1016/j.jaridenv.2020.104336

Li, L., Su, H., Du, Q., Wu, T., 2021. A novel surface water index using local background information for long term and large-scale Landsat images. ISPRS J. Photogramm. Remote Sens. 172. https://doi.org/10.1016/j.isprsjprs.2020.12.003

Lopes, P., 2009. Assessment of statistical downscaling methods – application and comparison of two statistical methods to a single site in Lisbon. IOP Conf. Ser. Earth Environ. Sci. 6. https://doi.org/10.1088/1755-1307/6/2/022015

Mahmoudi, P., Rigi, A., Miri Kamak, M., 2019. Evaluating the sensitivity of precipitation-based drought indices to different lengths of record. J. Hydrol. 579. https://doi.org/10.1016/j.jhydrol.2019.124181

Meenu, R., Rehana, S., Mujumdar, P.P., 2013. Assessment of hydrologic impacts of climate change in Tunga-Bhadra river basin, India with HEC-HMS and SDSM. Hydrol. Process. 27. https://doi.org/10.1002/hyp.9220

Miryaghoubzadeh, M., Khosravi, A.S., Zabihi, M., 2019. A Review of Drought Indices and their Performance. J. of Water and Sustainable Development. Volume 6, No.1. Pages 103 to 112. (In Persian)

Mohamadian, A., Kouhi, M., Adineh Baigi, A., Rasouli, S.J., Bazrafshan, B., 2010. Comparison of Monitoring of Drought Using SPI, DI and PNI and Zoning Them (Case study: Northern Khorasan Province). J. of Water and Soil Conservation. Vol. 17(1). (In Persian)

Mohseni, O., Stefan, H.G., Erickson, T.R., 1998. A nonlinear regression model for weekly stream temperatures. Water Resour. Res. 34. https://doi.org/10.1029/98WR01877

Morid, R., Shimatani, Y., Sato, T., 2020. An integrated framework for prediction of climate change impact on habitat suitability of a river in terms of water temperature, hydrological and hydraulic parameters. J. Hydrol. 587. https://doi.org/10.1016/j.jhydrol.2020.124936

Morid, S., Smakhtin, V., Bagherzadeh, K., 2007. Drought forecasting using artificial neural networks and time series of drought indices. Int. J. Climatol. 27. https://doi.org/10.1002/joc.1498

Ogunrinde, A.T., Oguntunde, P.G., Olasehinde, D.A., Fasinmirin, J.T., Akinwumiju, A.S., 2020. Drought spatiotemporal characterization using self-calibrating Palmer Drought Severity Index in the northern region of Nigeria. Results Eng. 5. https://doi.org/10.1016/j.rineng.2019.100088

Rajabi, A., Dev, S.S.-J.E.R., 2012, U., 2012. Climate index changes in future by using SDSM in Kermanshah, Iran. J. Environ. Res. Dev. 7.

Rehana, S., Sireesha Naidu, G., 2021. Development of hydro-meteorological drought index under climate change – Semi-arid river basin of Peninsular India. J. Hydrol. 594. https://doi.org/10.1016/j.jhydrol.2021.125973

Rezvanfar, I., Heidarzadeh, N., 2017. Investigating the effects of climate change on the area of Iran's wetland using remote sensing (Arjan wetlands). Master thesis, Kharazmi University, Tehran, Iran.

Sadeghi, M., Raisi Ardakani, E., 2018. Investigation of factors affecting the drying of Arjan wetland. 15th conference of Geological Society of Iran, Tehran. https://civilica.com/doc/135217 (In Persian)

Salajegheh, A., Rafiei Sardoii, E., Moghaddamnia, A., Malekian, A., Araghinejad, Sh., Khalighi Sigarodi, Sh., Saleh Pourjam, A., 2016. Performance assessment of LARS-WG and SDSM downscaling models in simulation of precipitation and temperature. Iran water and soil Res.Volume 48, NO.2. 253-262. (In persian)

Sarp, G., Ozcelik, M., 2017. Water body extraction and change detection using time series: A case study of Lake Burdur, Turkey. J. Taibah Univ. Sci. 11. https://doi.org/10.1016/j.jtusci.2016.04.005

Satish Kumar, K., Venkata Rathnam, E., Sridhar, V., 2021. Tracking seasonal and monthly drought with GRACE-based terrestrial water storage assessments over major river basins in South India. Sci. Total Environ. 763. https://doi.org/10.1016/j.scitotenv.2020.142994

Schnorbus, M.A., Cannon, A.J., 2014. Statistical emulation of streamflow projections from a distributed hydrological model: Application to CMIP3 and CMIP5 climate projections for British Columbia, Canada. Water Resour. Res. 50. https://doi.org/10.1002/2014WR015279

Shagega, F.P., Munishi, S.E., Kongo, V.M., 2019. Prediction of future climate in Ngerengere river catchment, Tanzania. Phys. Chem. Earth 112. https://doi.org/10.1016/j.pce.2018.12.002

Sobhani, B., Eslahi, M., Babaeian, I., 2014. The efficiency of SDSM and LARS-WG statistical exponential microscale models in simulating meteorological variables in the catchment area of Lake Urmia. Natural Geography Res. Volume 47, Number 4, winter 2014, 499-516 pp. (In Persian)

Tan, M.L., Ibrahim, A.L., Yusop, Z., Chua, V.P., Chan, N.W., 2017. Climate change impacts under CMIP5 RCP scenarios on water resources of the Kelantan River Basin, Malaysia. Atmos. Res. 189. https://doi.org/10.1016/j.atmosres.2017.01.008

Tukimat, N.N.A., Ahmad Syukri, N.A., Malek, M.A., 2019. Projection the long-term ungauged rainfall using integrated Statistical Downscaling Model and Geographic Information System (SDSM-GIS) model. Heliyon 5. https://doi.org/10.1016/j.heliyon.2019.e02456

Vrochidou, A.E.K., Tsanis, I.K., Grillakis, M.G., Koutroulis, A.G., 2013. The impact of climate change on hydrometeorological droughts at a basin scale. J. Hydrol. 476. https://doi.org/10.1016/j.jhydrol.2012.10.046

Wells, N., Goddard, S., Hayes, M.J., 2004. A self-calibrating Palmer Drought Severity Index. J. Clim. 17. https://doi.org/10.1175/1520-0442(2004)017<2335:ASPDSI>2.0.CO;2

Wen, Z., Zhang, C., Shao, G., Wu, S., Atkinson, P.M., 2021. Ensembles of multiple spectral water indices for improving surface water classification. Int. J. Appl. Earth Obs. Geoinf. 96. https://doi.org/10.1016/j.jag.2020.102278

Yang, H., Wang, Z., Zhao, H., Guo, Y., 2011. Water body extraction methods study based on RS and GIS, in: Procedia Environmental Sciences. https://doi.org/10.1016/j.proenv.2011.09.407

Zhang, F.F., Zhang, B., Li, J.S., Shen, Q., Wu, Y., Song, Y., 2011. Comparative analysis of automatic water identification method based on multispectral remote sensing, in: Procedia Environmental Sciences. https://doi.org/10.1016/j.proenv.2011.12.223

Zhao, C., Brissette, F., Chen, J., Martel, J.L., 2020. Frequency change of future extreme summer meteorological and hydrological droughts over North America. J. Hydrol. 584. https://doi.org/10.1016/j.jhydrol.2019.124316

6. Statements and Declarations

6.1. Funding

The authors declare that no funds, grants, or other supports were received during the preparation of this manuscript.

6.2. Competing Interests

The authors have no relevant financial or non-financial interests to disclose.

6.3. Author Contributions

"All authors contributed to the study conception and design. Material preparation, data collection and analysis were performed by Mahdiyeh Eghbal, and Nima Heidarzadeh. The first draft of the manuscript was written by Negar Esmaeili and all authors commented on previous versions of the manuscript. All authors read and approved the final manuscript."

6.4. Data Availability

The data that support the findings of this study are available from the corresponding author upon reasonable request.